Use of past satellite imagery to model algal dynamics in bays, estuaries and coastal ponds

Final report

Texas Water Development Board and was funded by the Research and Planning Fund of the Texas Water Development Board, Contract # 0704830671.

Project title: Use of past satellite imagery to model algal dynamics in bays, estuaries and coastal ponds

P.I.: Mathew Leibold, Section of Integrative Biology, UT at Austin

Postdoc: Lisette N. de Senerpont Domis, Section of Integrative Biology, UT at Austin

Undergraduate research assistant: Jeff Scott, Section of Integrative Biology, UT at Austin

Project objective: To develop and evaluate the use of Landsat imagery combined with "wavelet" statistical methods as a means to determine and quantify the role of different water inputs (runoff, marine, riverine) on algal dynamics in esturaties, bays and coastal ponds in Texas and do so in a way that optimizes utility of such analyses to TWDB needs.

Project background: The Texas Water Development Board (TWDB) is charged with evaluating the consequences of altered water use on Texas ecosystems. To that end it is important that the best possible information be used in making such decisions. In this project we wanted to evaluate the utility of long-term satellite imagery from Landsat in combination with other data to assess how different forms of water inflows (riverine, marine, and local runoff) and associated inputs of nutrients and materials affect the dynamics of algal blooms in estuary, bay, and coastal pond ecosystems. Each of these three ecosystem types are affected differently by the three sources of water inflows allowing contrasts between them to reveal the relative roles of each input type. In principle it should be possible to identify the roles of these inputs using simple models of plant growth and relating these to nutrient inputs. However the issue is more complex because algal dynamics are also prone to showing cycles that depend on other factors such as consumer-resource oscillations with their grazers. While this makes inferences more difficult it is important to take these into account because this also allows an evaluation of how the ecosystem as a whole (including higher trophic levels) are affected by water inflows.

One way to study such dynamics is to use statistical methods that focus on such oscillations and then study how different forms of inputs including both the type and the occurrence of these inputs affect these oscillations. This requires reasonably comprehensive data sets over fairly long periods of time as well as sophisticated statistical methods that dissect the role of these factors on dynamics. Collecting the data from scratch has the problem that the analyses will not be possible until fairly far into the future (i.e. 5-10 years) and will be expensive. It is possible that currently available data from long-term satellite imagery can do this much more promptly and less expensively. Our goal was to evaluate if such data available from satellite monitoring can be used to conduct such studies in a way that useful to the TWDB.

Project overview

Acquisition of satellite images

Lisette N. de Senerpont Domis started working on the project on 5/1/2007. She started with making an inventory of all the satellite images available for the area of interest (Table 1) through Texas Synergy, the Texas View Remote Sensing Consortium and the United States Geological Survey (USGS) or the Global Land Cover facility at the University of Maryland (GLFC). The Texas Synergy project is one of several NASA-sponsored projects that promotes the use of NASA's Earth observing System (EOS) data and data products in the daily work of state, regional and local government. It is run from the offices of the Center for Space Research (C.S.R.) at the University of Texas at Austin. Contacts at the UT- C.S.R. are Gayla Mullins (in charge of the Texasview Landsat archive), Larry Teng (who has experimented with developing chlorophyll concentration products using data from the Ocean Color Monitor (OCM) satellite for the Texas coast) and Theresa Howard (Mid-American Geospatial Information Center (MAGIC) program coordinator).

Table 1: Overview of satellite images available for the area of interest, including sensor characteristics and evaluation of the utility of the images for the current project.

Satellite Sensor	Spatial resolution	Spectral resolution	Temporal resolution	Period	Pro's	Con's
MODIS Aqua/ Seawifs	1 km, 4 km, 9 km,	36 bands	Daily, 8-daily, monthly, yearly	July 2002-present	Chlorophyll data are readily available (Ocean Color products) with a high temporal resolution	Poor spatial resolution, image quality varies due to sun glint and clouding, currently not georeferenced
OCM	350 m	8 bands	Daily	April 1999-present	High temporal resolution, moderate spatial resolution	Chlorophyll algorithms in developmental stage
Landsat 5TM/ 7ETM	15m, 30m, 60m	7 (TM) 8 (ETM)	16-daily	March 1984-present	High spatial resolution, high image quality, images are georeferenced	Poor spectral resolution requires test of different algorithms, limited images freely available

Selection of study area and images:

In the original research proposal we focused on the use of Landsat images, given its high spatial resolution and potential moderate temporal resolution. After the initial

drawback of finding only 5-10% of the archived Landsat images freely available for the areas of interests (i.e. path 25/row 39, path 25/row 40, path 26/row 40, path 26/row 41, path 26/row 42), we proceeded with selecting the Galveston Bay area (Fig. 1) as our main study area, given the relatively high number of images freely available (67 of which 9 are sliced off), the amount of ground truthing data available, (and the high number of Texas surface water and sediment quality stations (providing data on water chemistry, heavy metals, total suspended solids). In addition, the Galveston Bay area has a wide array of aquatic systems, differing in size and the type of water inflow (e.g. large freshwater reservoirs, bays, and estuaries). Although relatively small reservoirs are present in the area east of Galveston Bay (Fig.1.), the coastal ponds typical for Kenedy County (the original focal site) are absent in this area.

Through Dr. Antonietta Quigg (Department of Marine Biology, Texas A&M University) we were able to access three different sources of groundthruthing data: i.e. a data set authored by Dr. Jay Pickney (University of South Carolina) covering 6 stations in the Galveston bay from 1999-2002; a data set authored by Dr. Daniel Roelke and Dr. Stephen Davis of Tecas A&M University covering the same 6 stations in the Galveston bay from 2005-2006, and data from the Texas Commission on Environmental Quality and the Clean Rivers, collected from 1969-2006 (data set maintained by Lisa Gonzalez of the Houston Advanced Research Center). An overview of the Landsat images useable for time series analyses and the groundtruthing data available for part of these images (including the source) is presented in Table 2. All these images were acquired by either the Landsat 5 thematic mapper (TM) sensor, or by the Landsat 7 enhanced thematic mapper plus (ETM+) sensor. Landsats 5 and 7 orbit at an altitude of 705 km, and each provides a 16-day, 233-orbit cycle. The two satellite orbits are offset, allowing 8-day repeat coverage. These satellites were also designed to collect data over a 185-km swath. Both the TM sensor and the ETM+ sensor operate in seven spectral bands, which differ in spectral resolution and the potential use for this study (Table 3)

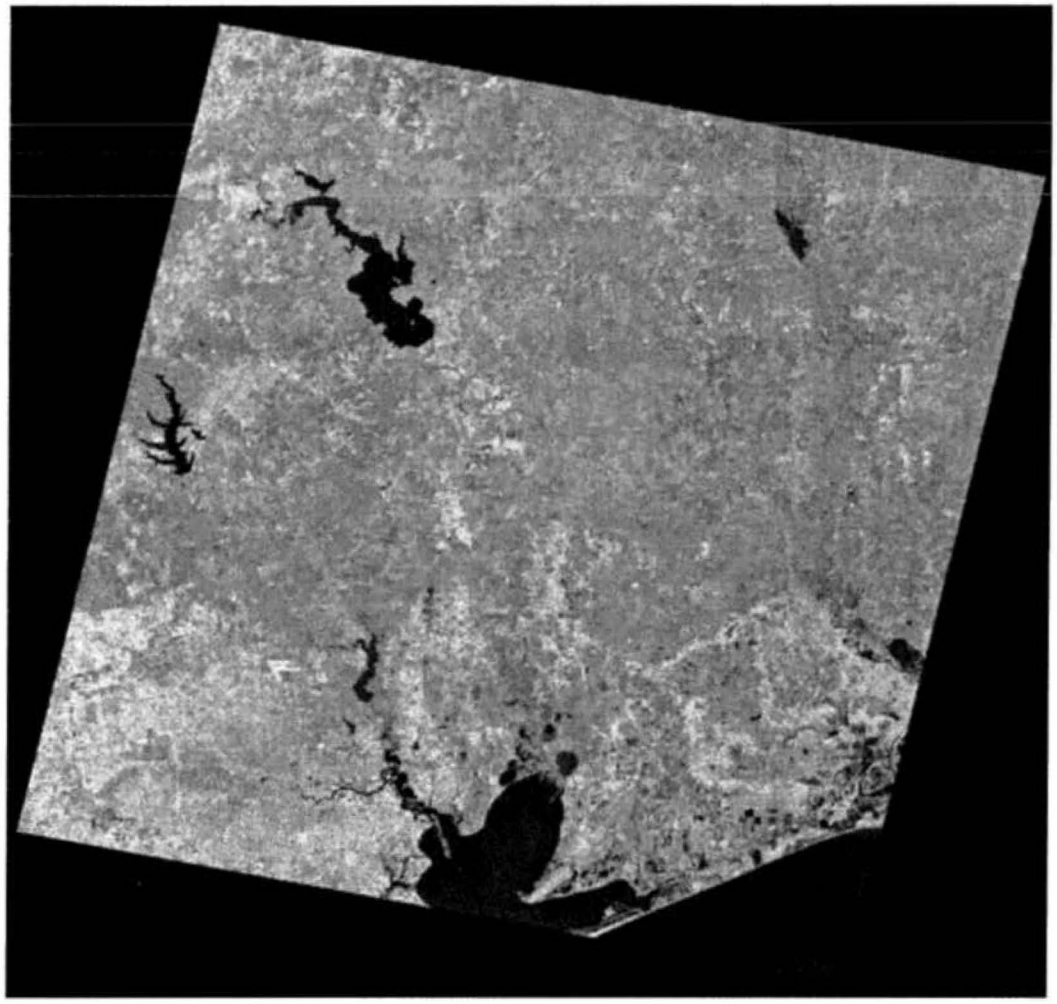

Figure 1: Landsat image of oath 25, Row 39, taken on 5/4/2005, source: United States Geological Survey

Table 3: Overview of images that will be used for timeseries analyses. Images were both chlorophyll and suspended matter data was available are used for ground truthing the respective chlorophyll/suspended matter models

Year	Julian day	Date	Sensor	Ground truthing data	Source
1984	310	05-11-1984	Landsat 5		
1984	342	07-12-1984	Landsat 5		
1985	8	08-01-1985	Landsat 5		
1986	27	27-01-1986	Landsat 5	Chlorophyll/ Suspended matter	TCEQ[1]
1989	339	05-12-1989	Landsat 5	Chlorophyll/ Suspended matter	TCEQ[1]
1993	30	30-01-1993	Landsat 5		
1994	97	07-04-1994	Landsat 5		
1994	353	19-12-1994	Landsat 5		
1997	25	25-01-1997	Landsat 5		
1997	361	27-12-1997	Landsat 5		
1998	300	27-10-1998	Landsat 5		

Year	Julian day	Date	Sensor	Ground truthing data	Source
1998	364	30-12-1998	Landsat 5		
1999	263	20-09-1999	Landsat 7		
1999	279	06-10-1999	Landsat 7	Chlorophyll/ Suspended matter	TCEQ[1]
1999	295	22-10-1999	Landsat 7		
1999	311	07-11-1999	Landsat 7	Chlorophyll/ Suspended matter	Texas A&M University[2]
1999	350	16-12-1999	Landsat 7	Chlorophyll/ Suspended matter	Texas A&M University[2]
2000	10	10-01-2000	Landsat 7		
2000	34	03-02-2000	Landsat 5		
2000	58	27-02-2000	Landsat 7		
2000	202	20-07-2000	Landsat 7	Chlorophyll/ Suspended matter	Texas A&M University[2]
2000	274	30-09-2000	Landsat 5		
2000	314	09-11-2000	Landsat 7		
2001	116	26-04-2001	Landsat 5	Chlorophyll/ Suspended matter	TCEQ[1]
2001	268	25-09-2001	Landsat 7	Chlorophyll/ Suspended matter	Texas A&M University[2]
2002	15	15-01-2002	Landsat 7		
2002	63	04-03-2002	Landsat 7		
2002	135	15-05-2002	Landsat 5	Chlorophyll/ Suspended matter	TCEQ[1]
2002	215	03-08-2002	Landsat 5		
2003	2	02-01-2003	Landsat 7		
2003	18	18-01-2003	Landsat 7		
2003	82	23-03-2003	Landsat 7		
2003	266	23-09-2003	Landsat 5	Chlorophyll/ Suspended matter	TCEQ[1]
2004	125	04-05-2004	Landsat 5	Chlorophyll/ Suspended matter	TCEQ[1]
2004	253	09-09-2004	Landsat 5		
2004	349	14-12-2004	Landsat 5	Chlorophyll/ Suspended matter	TCEQ[1]
2005	303	30-10-2005	Landsat 5	Chlorophyll/ Suspended matter	TCEQ[1]
2006	18	18-01-2006	Landsat 5		
2006	178	27-06-2006	Landsat 5		
2006	290	17-10-2006	Landsat 5		

1 [1]Contact person: lgonzalez@harc.edu

2 [2]Contact person: jpinckney@biol.sc.edu

Table 3: Characteristics of Landsat channels and potential use

Channel (TM/ETM+)	Band	Waveband (μm)	Use
1	Blue	0.45-0.515	Useful for bathymetric mapping ,soil and vegetation discrimination
2	Green	0.525-0.605	Vegetation discrimination and vigor assessment, water quality assessment (chlorophyll and sediment)
3	Red	0.63-0.69	Near-surface information on sediment and chlorophyll concentrations
4	Near-Infrared	0.75-0.90	Delineating water features, assessing turbidity
5	Short-wave infrared	1.55-1.75	Distinguishing clouds from snow and ice
6	Thermal infrared	10.4-12.5	Water temperature and soil moisture
7	Short wave infrared	2.08-2.35	Mapping hydrothermally altered rocks associated with mineral deposits

Image calibration and standardization

All of the acquired images were at least systematic corrected, implying that radiometric and geometric correction was derived from data collected systematically by the sensor and spacecraft. Certain scenes had even higher geometric accuracy, as the United States Geological Survey incorporated ground control points and a digital elevation model for topographic accuracy. All additional image restoration, rectification (both radiometric and geometric), and indices calculation operations were carried out in Erdas Image V9.1 (Leica Geosystems Geospatial imaging). Of the available 67 satellite images (both Landsat 5 TM and Landsat 7 ETM covering a time span of 1984-2007) 27 images are of lesser quality, either due to severe clouding/sun glint, or due to presence of striping (a consequence of the permanent failure of the Scan Line Corrector of Landsat 7 ETM (as of May 31, 2003).

Reprojection: The images originated from four different sources: Columbia Center regional geospatial service center; the USGS Global Visualization Viewer (GLOVIS); the Global Land Cover Facility (GLCF) at the University of Maryland; and the Center for Space Research (C.S.R.) at the University of Texas at Austin. As they had different projections, they had to be reprojected into the same pixel size and map projections. We resampled these images to 30 x 30m grid spacing and map projection WGS 84, UTM zone 15, using the nearest neighbor method with polynomial approximation. The maximum polynomial order allowed for polynomial approximation was three,

whereas the tolerance for polynomial approximation as expressed in root mean square error (RMSE) was set on 0.1 pixels per image. In those cases where tolerance was exceeded, we chose to continue to use polynomial approximation with the solution which has the lowest RMSE. We chose nearest neighbor resampling as it retains the original pixel value (Aronoff 2005).

Geometric correction: To achieve the high geographic accuracy necessary for mulititemporal image analyses the images were rectified on an image-to-image basis. Thus, all images were co-registered to the Landsat 5 TM images of 5/4/2005 with a root mean square error of less than 0.5 pixels per image, using a second order polynomial with at least 25 Ground Control Points (Wilson and Sader 2002). We chose this scene for co-registration as it was completely cloud free and had the highest level of procession (i.e. terrain corrected) provided by the United States Geological Survey. In addition, groundtruthing data was available for that image.

Radiometric correction: Radiance measured by a sensor is affected by differences in sun illumination, viewing geometry, atmospheric effects and instrument calibration. The resulting errors in sensor output are to a certain extent compensated by systematic radiometric correction of each band derived from the data from the sensor and space craft. These additive errors become even more significant when using multitemporal data. To correct for the degradation of image quality we had to resort to image-based radiometric correction methods, as we did not have in-situ atmospheric measurements nor radiometric transfer code on the date of image acquisition. For our image-based radiometric correction, two different methods were used and compared:

1. Digital number to reflectance conversion: The Landsat sensor typically measures the total radiance reflected from a particular ground target; subsequently converts it to a digital number (DN or voltage measurements) and transmits it to the ground stations. These 8-bit satellite-quantize calibrated digital numbers of the images are converted to at-sensor reflectance by normalizing for the solar elevation angle (Chavez 1996; Markham and Barker 1986). This form of radiometric correction assumes a Lambertian surface under cloudfree conditions, and can therefore be used a null-model for models that remove atmospheric effects (see below). The equation is as follows:

$$\rho_\lambda BandN = \pi((([DN]_\lambda bandN * G_\lambda bandN + B_\lambda bandN)) / (E_\lambda bandN * \cos((90 - \theta) * \pi/180))) * D^2$$

Where,

ρ_{BandN} = At-satellite Reflectance for Band N (unitless)

DN_{bandN} = Digital Number for Band N

G_{bandN} = Gain band N (DN)

B_{bandN} = Bias band N (DN)

D = Normalized Earth-Sun Distance (astronomical units), function of date

E_{bandN} = Solar exoatmospheric Irradiance for Band N (mW cm^{-2} μm^{-1})

θ = Solar elevation (degrees)

To account for the impact of sensor degradation on gain parameters we followed the approach described by Schroeder et al. (2006).

2. Dark Object Substraction - Cosine approximation (DOS-COST): This is a combination of the Dark Object Substraction or DOS model (Chavez 1988) and Cosine estimation of atmospheric transmittance or COST model (Chavez 1996) and in addition to radiometric calibration, removes atmospheric effects from the image. The DOS model is based on the assumption that within satellite images there exist features that have near-zero reflectance (e.g. asphalt, shadow). Consequently, the signal recorded by the sensor is proportional to atmospheric scattering or path radiance, and can be used to account for degradation of image quality caused by the atmospheric scattering. In the COST Model, a second order cosine function is used to approximate atmospheric transmittance. In a comparison of different atmospheric correction model, Chavez et al (1996) reported that the combination of the DOS and COST model can compute reflectances values comparable to results with complex radiative transfer models using in situ atmospheric measurements. The equation is as follows:

$$\rho_{\lambda}BandN = \pi((\lfloor DN \rfloor_{\lambda}bandN * G_{\lambda}bandN + B_{\lambda}bandN) - (\lfloor DNdark \rfloor_{\lambda}bandN * G_{\lambda}bandN + B_{\lambda}bandN))/(E$$

Where,

ρ_{BandN} = At-satellite Reflectance for Band N (unitless)

DN_{bandN} = Digital Number for Band N

G_{bandN} = Gain band N (DN)

B_{bandN} = Bias band N (DN)

$DNdark_{bandN}$ = Digital Number representing Dark Object for Band N

D = Normalized Earth-Sun Distance (astronomical units)

E_{bandN} = Solar exoatmospheric Irradiance for Band N (mW cm^{-2} μm^{-1})

θ = Solar elevation (degrees)

τ = Atmospheric transmittance expressed as $\cos((90 - \theta) * \pi/180))$

To account for the impact of sensor degradation on gain parameters we followed the approach described by Schroeder et al. (2006).

.

The 40 images of good to high quality have been coregistered and atmospherically corrected.

Chlorophyll algorithms:

Lisette de Senerpont Domis developed a total of 14 chlorophyll retrieval models based on (adaptations) of existing algorithms (Table 4). In addition, to evaluate the effect of suspended matter on chlorophyll retrieval she developed two turbidity models as well (Table 4).

Table 4: Overview of algorithms used to retrieve chlorophyll and suspended matter estimates from Landsat images. TMx stands for (enhanced)Thematic Mapper band x. ETM stands for enhanced Thematic Mapper plus.

Response parameter	Model	Reference

Response parameter	Model	Reference
Chlorophyll	$\frac{TM1 - TM3}{TM2}$	Mayo et al. (1995)
Chlorophyll	$\frac{TM4}{TM1 + TM2 + TM4}$	Lindell et al. (1999)
Chlorophyll	$\frac{TM2}{TM3}$	Ekstrand (1992)
Chlorophyll	$\frac{TM4}{TM2}$	
Chlorophyll	$\frac{TM3}{TM1}$	Braga et al. (2003)
Chlorophyll	$\frac{TM4}{TM3}$	
Chlorophyll	$\frac{TM4 - TM3}{TM4 + TM3}$	Normalized Vegetation Index (Tucker 1979)
Chlorophyll	$\frac{TM4 - TM3}{TM4 + TM3 + 0.5}$	Soil-adjusted Vegetation Index (Huete 1988)
Chlorophyll	$2.5 * \frac{TM4 - TM3}{1 + tm4 + 6.0 * TM3 - 7.5 * TM1 + 1}$	Enhanced Vegetation Index (Liu and Huete 1995)
Chlorophyll	$\left(\frac{2 * TM4 + 1 - \sqrt{(2 * TM4)} + 1 - 8 * (TM4 - TM3)}{2}\right)^2$	Modified Soil Adjusted Vegetation Index
Chlorophyll	$\frac{(TM5 - TM3)}{((TM5 + TM3 + 0.1) * 1.1)} - \frac{TM6}{2}$	Soil Adjusted Total Vegetation Index (Marsett et al. 2006)
Suspended matter	$\frac{TM1}{TM1 + TM2 + TM3}$	

Response parameter	Model	Reference
Suspended matter	$TM3 - TM4$	
Chlorophyll/suspended matter	Brightness = *0.356(ETM1) + 0.3972(ETM2) + 0.3904 (ETM3) + 0.6966 (ETM4) + 0.2286 (ETM5) + 0.1596 (ETM7)*	Tasseled Cap transformation for ETM+ data (Huang et al. 2002)
	Greenness = *-0.3344 (ETM1) -0 3544 (ETM2) – 0.4556 (ETM3) + 0.6966 (ETM4) -0.02420(ETM5) -0 .2630 (ETM7)*	
	Wetness = *0.2626 (ETM1) + 0.2141 (ETM2) + 0.0926 (ETM3) + 0.0656 (ETM4) - 0 .7629(ETM5) -0 .5388 (ETM7)*	
	Haze = *0.0805 (ETM1) - 0.0498 (ETM2) - 0.1950 (ETM3) – 0.1327 (ETM4) - 0.5752(ETM5) + -0.7775 (ETM7)*	
Chlorophyll/suspended matter	Brightness = *0.2043(TM1) + 0.4158(TM2) + 0.5524 (TM3) + 0.5741 (TM4) +0.3124 (TM5) + 0.2303 (TM7)*	Tasseled Cap transformation for TM data (Crist and Cicone 1984; Crist and Kauth 1986)
	Greenness = *-0.1063(TM1) -0 .2819 (TM2) - 0.4934 (TM3) + 0.7940 (TM4) -0 .0002 (TM5) -0 .1446 (TM7)*	
	Wetness = *0.0315 (TM1) + 0.2021 (TM2) + 0.3102 (TM3) + 0.1594 (TM4) - 0 6806 (TM5) -0 6109 (TM7)*	
	Haze = *-0.2117 (TM1) - 0.0284 (TM2) - 0.1302 (TM3) - 0.1007 (TM4) + 0.6529(TM5) - 0.7078 (TM7)*	

Developed for use with Landsat data, the Tasseled Cap transformation (Crist and Cicone 1984; Crist and Kauth 1986; Huang et al. 2002) is essentially a guided and scaled principal components analysis, which compresses the 6 Landsat TM or ETM+ bands into 4 bands. These four resulting components typically represent "brightness"; "greenness"; "wetness"; and "haze" of an image.
It seems to be the most promising model, taking different aspects of water quality into account. All models are run on both the digital number to reflectance conversion atmospheric correction model as well as the DOS-COST atmospheric correction model to be able to evaluate the usefulness of these atmospheric correction models.

Ground truthing data:

In September 2008, Lisette de Senerpont Domis and Mathew Leibold had a meeting with both scientists from University of Texas at Port Aransas (James McClelland) and from Texas A&M University (Antonietta Quigg and Daniel Roelke) to talk about

available datasets for testing our chlorophyll retrieval algorithms. Making use of the extensive Galveston Bay study network of Dr. Antonietta Quigg, we gained access to chlorophyll and suspended matter data of Dr. Pinckney (former Texas A&M University, time period 1999-2002); Dr. Davis and Roelke (Texas A&M University, time period 2005-2006), Lisa Gonzalez (HARC, time period 1984-2006), and data from the TPWD (via Ruben Solis, time period 1976-2005). In addition, Ruben Solis provided both daily meteorological data from the National Climatic Data Center and water quality data for the time period and area under study. All these data are formatted into an easy to use Microsoft Access database. For 13 images (of a total of 40) ground truthing data is available for both chlorophyll and suspended matter estimates (Table 2). These data will be used to validate the different chlorophyll and suspended matter models. At present the data is not groundtruthed, as the chlorophyll and suspended solids data needed to be georeferenced using Geographical Information System (GIS) analysis (see below).

GIS analyses

Currently, different layers are being created in ARCGIS of the available data on chlorophyll, suspended matter and meteorological data. This will allow for ground truthing of the satellite image, taking into account prevailing weather conditions. Originating from four different sources, we have to georeference the data available for ground truthing. The majority of the data available is for the Galveston bay area only, hampering good ground truthing of other water bodies in the path 25/ row39 image. As most of the data on environmental variables also focuses on the Galveston bay area, most likely we will proceed by concentrating our time series analyses on both environmental and chlorophyll data on the Galveston Bay area.

Conclusions:

Landsat images are of somewhat limited utility for long term monitoring of chlorophyll dynamics. First, while there are many images taken, only a small portion of these are readily available at low expense. Acquiring images outside the ones freely available requires purchasing them through USGS. A terrain corrected image, having the level of correction which we need for our subsequent analyses would cost $500 (Landsat 5) to $640 (Landsat 7) per scene. In addition, a good proportion (roughly 1/3) of these are not useful due to cloud cover or sun glint. Finally the work needed to calibrate and standardize these images is high (roughly 4 hours/image). Only after these initial processing steps are undertaken, chlorophyll modeling and subsequent GIS analyses can take place. As a consequence, the frequency and spatial and spectral resolution of the data can be used in time series analysis but just barely. This means that they could be used to examine large trends and effects but probably not be useful in detailed work.

Additional work needed

At this point, we have 40 images, 13 of which have ground truthing data associated with them. These have been radiometrically corrected and geometrically corrected and the different algorithms listed in Table 4 have been executed. Our

next step is to evaluate the different model outcome using the available ground truth data in GIS analysis. This will allow us to select one (or two) algorithms to use for future work. The next step is to run an initial time series analyses on the 40 images, and to check for the presence of long-term trends. We will test for long-term trends, for short term associations with climate and water flow data, and for oscillations using wavelets or fourier analyses. This allows us to identify how much temporal resolution and time series length are needed to get significant results and to evaluate future work to obtain missing Landsat images) are warranted.

Whereas most remote sensing studies use a rather low number (typical up to 5) of images on a yearly interval, our study stands out by using a large number of images (40), with multiple data points per year. In addition, using time series analyses, such as wavelet analyses on these types of data is innovative as well.

References:

Aronoff, S. 2005. Remote sensing for GIS manages. ESRI Press.

Braga, C. Z. F., M. L. Vianna, and B. Kjerfve. 2003. Environmental characterization of a hypersaline coastal lagoon from Landsat-5 Thematic Mapper data. Int. J. Remote Sens. **24:** 3219-3234.

Chavez, P. S. 1988. An improved dark-object substraction technique for atmospheric scattering correction of multispectral data. Remote Sensing of Environment **24:** 459-479.

---. 1996. Image-based atmospheric corrections revisited and improved. Photogramm. Eng. Remote Sens. **62:** 1025-1036.

Crist, E. P., and R. C. Cicone. 1984. A physically-based transformation of thematic mapper data-the TM Tasseled Cap. IEEE Trans. Geosci. Remote Sensing **22:** 256-263.

Crist, E. P., and R. J. Kauth. 1986. The tasseled cap de-mystified. Photogramm. Eng. Remote Sens. **52:** 81-86.

Ekstrand, S. 1992. Landsat TM based quantification of chlorophyll-a during algal blooms in coastal waters. Int. J. Remote Sens. **13:** 1913-1926.

Huang, C., B. Wylie, L. Yang, C. Homer, and G. Zylstra. 2002. Derivation of a tasselled cap transformation based on Landsat 7 at-satellite reflectance. Int. J. Remote Sens. **23:** 1741-1748.

Huete, A. R. 1988. A soil-adjusted vegetation index (SAVI). Remote Sensing of Environment **25:** 295-309.

Lindell, T., D. Pierson, G. Premazzi, and E. Ziholi. 1999. Manual for monitoring European Lakes using remote sensing techniques.

Liu, H. Q., and A. Huete. 1995. A feedback based modification of the NDVI to minimize canopy background and atmospheric noise. IEEE Trans. Geosci. Remote Sensing **33:** 457-465.

Markham, B. L., and J. L. Barker. 1986. Landsat MSS and TM post-calibration dynamic ranges, exoatmospheric reflectances and at-satellite temperatures. EOSAT Landsat Technical Notes **1:** 3-8.

Marsett, R. C. and others 2006. Remote sensing for grassland management in the arid Southwest. Rangeland Ecology & Management **59:** 530-540.

Mayo, M., A. Gitelson, Y. Z. Yacobi, and Z. Benavraham. 1995. Chlorophyll distribution in Lake Kinneret determined from Landsat Thematic Mapper Data. Int. J. Remote Sens. **16:** 175-182.

Schroeder, T. A., W. B. Cohen, C. H. Song, M. J. Canty, and Z. Q. Yang. 2006. Radiometric correction of multi-temporal Landsat data for characterization of early successional forest patterns in western Oregon. Remote Sensing of Environment **103:** 16-26.

Tucker, C. J. 1979. Red and photographic infrared linear combinations for monitoring vegetation. Remote Sensing of Environment **8:** 127-150.

Wilson, E. H., and S. A. Sader. 2002. Detection of forest harvest type using multiple dates of Landsat TM imagery. Remote Sensing of Environment **80:** 385-396.